Human Pathology (2021) **107**, 104–116

ELSEVIER

Human PATHOLOGY

www.elsevier.com/locate/humpath

Original contribution

Genotype-phenotype associations in colorectal adenocarcinomas and their matched metastases☆,☆☆,☆☆☆

Kyriakos Chatzopoulos MD [a,b,*,1,2], Vassiliki Kotoula MD, PhD [a,b,2], Georgia-Angeliki Koliou MSc [c], Eleni Giannoulatou PhD [d,e], Kyriaki Papadopoulou PhD [a], Vasilios Karavasilis MD, PhD [f], Elissavet Pazarli MD [g], Stavroula Pervana MD [g], Georgia Kafiri MD, PhD [h], Georgios Tsoulfas MD, PhD [i], Sofia Chrisafi PhD [a], Helen Sgouramali MSc [a], Pavlos Papakostas MD [j], Dimitrios Pectasides MD, PhD [j], Prodromos Hytiroglou MD, PhD [b], George Pentheroudakis MD, PhD [k,l], George Fountzilas MD, PhD [a,m,n]

[a] *Laboratory of Molecular Oncology, Hellenic Foundation for Cancer Research/Aristotle University of Thessaloniki, Thessaloniki, 54124, Greece*
[b] *Department of Pathology, Aristotle University of Thessaloniki, School of Health Sciences, Faculty of Medicine, Thessaloniki, 54124, Greece*
[c] *Section of Biostatistics, Hellenic Cooperative Oncology Group, Data Office, Athens, 11524, Greece*
[d] *Computational Genomics Laboratory, Victor Chang Cardiac Research Institute, Darlinghurst, NSW, 2010, Australia*
[e] *The University of New South Wales, Kensington, NSW, 2052, Australia*
[f] *Department of Medical Oncology, Papageorgiou Hospital, Aristotle University of Thessaloniki, School of Health Sciences, Faculty of Medicine, Thessaloniki, 56403, Greece*
[g] *Department of Pathology, Papageorgiou Hospital, Aristotle University of Thessaloniki, School of Health Sciences, Faculty of Medicine, Thessaloniki, 56403, Greece*
[h] *Department of Pathology, Hippokration Hospital, Athens, 11527, Greece*
[i] *Department of Surgery, Aristotle University of Thessaloniki, Thessaloniki, 54124, Greece*

Abbreviations: TILs, tumor-infiltrating lymphocytes; FFPE, formalin-fixed paraffin-embedded; HeCOG, Hellenic Cooperative Oncology Group; AJCC, American Joint Committee on Cancer; H&E, Hematoxylin and eosin; TCC, Tumor Cell Content; NGS, Next-generation sequencing; MAF, Minor allele frequency; VAF, Variant allele frequency; MMR, Mismatch repair; VUS, Variant of unknown significance; SNP, Single-nucleotide polymorphism; OS, Overall survival; CNA, Copy number alteration.

☆ Dedicated to the memory of Ioannis Efstratiou, pathologist and friend.

☆☆ Competing interests: None.

☆☆☆ Funding/Support: This work was supported by a grant from the Hellenic Cooperative Oncology Group (HeCOG) [HE TRANS_CRC] and institutional funds from the Department of Pathology of the Aristotle University of Thessaloniki. The funders have not played any role in research design or implementation.

E-mail address: Chatzopoulos.Kyriakos@mayo.edu (K. Chatzopoulos).

[1] Present address: Department of Laboratory Medicine and Pathology, Mayo Clinic, 55905, Rochester, MN, United States of America.

[2] The first two authors contributed equally to this work.

https://doi.org/10.1016/j.humpath.2020.10.009

[j] *Oncology Section, Second Department of Internal Medicine, Hippokration Hospital, Athens, 11527, Greece*
[k] *Department of Medical Oncology, Medical School, University of Ioannina, Ioannina, 45500, Greece*
[l] *Society for Study of Clonal Heterogeneity of Neoplasia (EMEKEN), Ioannina, Greece*
[m] *Aristotle University of Thessaloniki, Thessaloniki, Greece*
[n] *German Oncology Center, Limassol, Cyprus*

Received 20 July 2020; revised 3 October 2020; accepted 30 October 2020

Available online 5 November 2020

Keywords:
Colorectal neoplasms;
Neoplasm metastasis;
Clonal evolution;
Lymphocytes;
Tumor-infiltrating;
Necrosis;
Next-generation sequencing

Summary Although primary colorectal carcinomas (CRCs) frequently share genetic alterations with their metastases, morphologic surrogates reflecting the genotype contexture of metastases remain largely unknown. We investigated phenotype/genotype associations in paired primary and metastatic colorectal adenocarcinomas from 75 patients. Thirty-three (44%) metastatic lesions were synchronous and 42 (56%) were metachronous. Tumor budding, micronecrosis, and tumor-infiltrating lymphocyte (TIL) density were compared with matched next-generation sequencing genotypes. Micronecrosis in the primary were significantly associated with nodal status ($P = 0.0054$) and with micronecrosis in metastatic sites ($P = 0.0216$), particularly in metachronous metastases ($P = 0.0033$). With a 57-gene panel, one or more mutations were identified in 64 (85.3%) cases. In metastases, high (brisk) TILs were associated with overall mutational burden ($P = 0.0058$) and with mutations in *EGF* ($P = 0.0325$), RAS genes ($P = 0.0043$), and MMR genes ($P = 0.0069$), whereas high-level micronecrosis correlated with mutations in *APC* ($P = 0.0004$) and *MSH6* ($P = 0.0385$) genes. Genomic alterations were shared in 90.1% of primary/metastatic pairs, but clonality of the same mutation was shared in only 57.1% of paired lesions. Compared with synchronous, metachronous metastases had more private clonal alterations ($P = 0.0291$); in this group, clonal alterations coincided with brisk TILs ($P = 0.0334$) and high micronecrosis ($P = 0.0133$). High TILs in metastatic lesions were predictive of favorable overall survival (log-rank $P = 0.044$). The observed phenotype/genotype associations favor the clonal evolution model in CRC metastases that seems accompanied by intense host immune response. If the role of micronecrosis and brisk TILs in metachronous metastases is validated in larger studies, these histologic parameters will be worth adding in the armamentarium for the evaluation of metastatic CRC.

1. Introduction

Colorectal adenocarcinoma is the third most common and second most lethal malignancy with approximately 880,000 annual deaths worldwide [1]. Although curable if diagnosed at an early stage, approximately 20% of patients present with metastatic disease and have a very poor prognosis with a 5-year survival rate of only 14% [2]. Even among patients without metastatic disease at presentation, approximately 19% will eventually develop distant metastases, most frequently to the liver [3]. Interestingly, a small minority of patients who develop metachronous metastases can be curatively treated with metastasectomies offering a 5-year OS of around 60% [3].

Advances in colorectal cancer research have elucidated facts about the pathogenesis of the disease, leading to a better understanding of the underlying molecular events and the identification of potentially targetable genomic alterations [4]. Histopathologic evaluation, however, remains of paramount importance, and key histopathologic findings may reflect a specific genomic setting, such as in the case of MMR-deficient tumors that frequently have brisk tumor-infiltrating lymphocytes (TILs) and lack the typical *dirty* necrosis of MMR-proficient colorectal carcinomas (CRCs) [5].

On this basis, and also because (a) some patients with colorectal tumors promptly present with metastatic disease, whereas others tend to develop metachronous metastases [3], and (b) some patients with metastatic disease have favorable outcomes, we compared molecular alterations with histologic features in primary CRCs and matched metastases. We hypothesized that morphologic/phenotypic features in either or both tumor sites may reflect characteristics of the underlying genotypes.

2. Materials and methods

2.1. Patients and tissues

Formalin-fixed paraffin-embedded (FFPE) tissue blocks of matched primary and distant metastatic tumors of the colon and rectum were retrieved from the repository of the Hellenic Cooperative Oncology Group (HeCOG). Corresponding patients had been diagnosed with colorectal cancer between 2003 and 2015 and had presented with stage IV disease (AJCC 8th edition) or had been initially diagnosed with colorectal cancer at stage II-III (nonstage IV) and developed metastatic disease after >3 months. Patients had been treated in HeCOG affiliated clinical centers or within adjuvant trials by HeCOG; all had provided informed consent for the use of their biologic material for research purposes. Adjuvant treatment included chemotherapy only; first-line treatment included chemotherapy or chemotherapy plus bevacizumab or chemotherapy plus anti-EGFR antibodies. The study was approved by the Bioethics Committee of the Aristotle University of Thessaloniki (AUTH, #356/15/7/2016). Patients had signed informed consent for the use of their biological material for research purposes. Peripheral blood samples were available for 65 patients. Primary tumors and synchronous metastatic samples were obtained before treatment administration. Metachronous metastatic samples were obtained upon administration of chemotherapy; such samples were obtained from both nonstage IV and stage IV patients.

2.2. Tissue processing and phenotyping

We examined 170 FFPE tissue blocks from 85 patients, 85 from the primary tumor and 85 from matched metastatic sites, along with the corresponding local hematoxylin and eosin (H&E) slides and histology reports. The blocks were centrally examined at the Laboratory of Molecular Oncology (MOL; Hellenic Foundation for Cancer Research/AUTH, Thessaloniki, Greece) for tissue adequacy and new H&E whole-section slides were evaluated for the following histological parameters: area marking for macrodissection and tumor DNA content (tumor cell content %), as described in the DATA MANUSCRIPT, budding in primary tumors, as well as TILs density and frequency of micronecrotic areas in both primary and metastatic sites. For TIL density, we incorporated the recommendations suggested by Hendry et al., thus reporting the area occupied by stromal TILs as percentage of the total tumor stromal area in both primary tumor and metastases [6,7].

We evaluated tumor budding on H&E sections of primary tumors and more specifically on a single hotspot (0.785 mm^2) of the invasive front with the most tumor buds, defined as single cells or clusters of up to 4 tumor cells. We reported buds as absolute counts per 0.785 mm^2. Multiple available H&E sections were evaluated under low magnification (×100), and the section with the highest number of buds was selected for further assessment, in accoradance with the consensus guidelines by Lugli et al. [8].

Micronecrosis was defined as a microscopic area (focus) of single or multiple necrotic cells disrupting the architecture of the malignant glandular structures and accompanied by neutrophilic inflammation on high magnification (×400), as opposed to massive confluent coagulative necrosis identifiable at low magnification (×40) [9]. Tumor necrosis has been traditionally semiquantitatively evaluated under low magnification (×40) in accordance with the method previously published by Pollheimer et al. [9]. We applied the same principle to evaluate micronecrosis under high magnification (×400) in accordance with the percentage of micronecrotic areas to the total viable and nonviable tumor cell area in hotspots identified after screening at intermediate magnification (×200).

Primary and metastatic tumors were also interrogated for MMR protein status with immunohistochemistry (IHC) for MLH1, PMS2, MSH2, and MSH6 protein expression, as previously described [10].

2.3. Genotyping

DNA samples were processed for next-generation sequencing (NGS) with the IAD47763_31 Ampliseq panel (Applied Biosystems/Thermo Fisher Scientific) in an Ion Torrent Proton sequencer (Thermo Fisher Scientific, Paisley, UK). The panel targets, NGS application, samples, and variant technical characteristics, criteria for variant and sample eligibility, as well as variant annotations, along with the entire data sets are available in the DATA MANUSCRIPT.

In total, 235 samples (170 FFPE and 65 germline DNA) were processed with NGS. After excluding ineligible samples and patients with incomplete clinical data, 141 FFPE tumor (71 primary, 70 metastatic sites) and 49 germline genotypes were considered for analysis (Fig. 1). With the applied criteria, primary/metastatic variants were comparable in tumors from 66 patients.

2.4. Statistical analysis

Histological parameters were analyzed as binary variables by using the median values as cutoffs for high/low categories. Low budding was considered for values 0−3 (high: ≥4); low primary and metastatic micronecrosis for values 0−9% (high: ≥10%); low primary and metastatic TILs for 0−19% density (high: ≥20%).

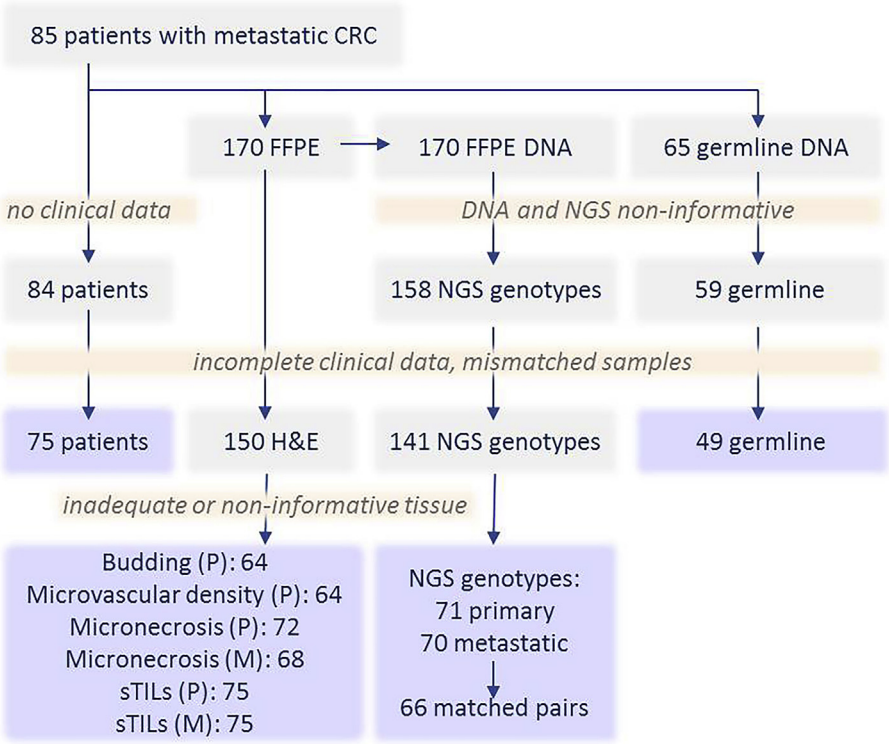

Fig. 1 Study design and REMARK diagram. Flowchart illustrating the case selection process for histopathologic evaluation and molecular testing. CRC, colorectal cancer; FFPE, formalin-fixed paraffin-embedded; NGS, next-generation sequencing; H&E, hematoxylin and eosin; P, primary; M, metastatic; sTILs, stromal tumor-infiltrating lymphocytes.

Mutations and mutated genes present in the primary and matched metastatic tumor were considered as shared mutations; mutations present in only one of the paired tumors were considered as private (private primary [P], private metastatic [M]). Mutations present in primary and matched metastatic tumors at clonal VAFs in either or both sites were considered as shared clonal; mutations at clonal VAFs present in one site only were considered as private clonal mutations (P or M). Clonal status was further examined as shared in primary and metastasis vs. all other instances (private clonality, private mutations, no mutations). Numbers of mutations and mutated genes, clonal, shared, and private mutations were examined as continuous variables. Mutations in high-prevalence genes (e.g., *APC*, *KRAS*) were examined as binary variables (nonmutant/mutant).

For descriptive variable comparisons classic tests were applied (chi-square, Wilcoxon rank-sum, Spearman's correlation). Because the number of patients was small and the cohort was heterogeneous with respect to main determinants of outcome in colorectal cancer (disease stage, metastasectomies and their timing, various treatment lines), we only examined the probability of OS, defined as the time from diagnosis to death or last follow-up (for patients alive and lost to follow-up), with log-rank testing. Statistical significance was set at 5%, and analysis was performed with SAS, version 9.3 (SAS Institute, Cary, NC) software.

3. Results

3.1. Clinical characteristics

Demographic and clinicopathologic data for the 75 patients with informative histological re-evaluation data and NGS tissue genotypes are presented in Table 1. Most patients had left sided, stage IV disease (detailed origin of the examined samples can be found in the DATA MANUSCRIPT). In the 22 nonstage IV patients, the median time to metastasis was 16.8 months (range: 5.1−79.2 months). In the 19 patients who received adjuvant treatment, the median time to diagnosis of metastasis was 9.7 months after treatment completion (range: 0.1−34.5 months). Based on patient clinical data and histology reports, metastasectomies were performed in 18 of 53 (34.0%) stage IV patients, and at relapse in 20 of 22 (90.1%) nonstage IV patients.

Importantly, in the 53 patients with stage IV disease, 20 of the examined metastatic tissues were obtained at time points ranging 5.8 months to >4 years after initial

Table 1 Selected patient and tumor characteristics.

Age at the time of first diagnosis (N:75)		
Median (Range)	62.63 (24.30–80.65)	
Age at metastasis (N:75)		
Median (Range)	64.70 (24.34–80.65)	
	N	**%**
Gender (N:75)		
Men	40	53.33
Women	35	46.67
Previous other cancer (N:71)		
No	61	85.92
Yes	10	14.08
Family cancer (N:64)		
No	30	46.88
Yes	34	53.12
Disease stage (AJCC 8th) (N:75)		
II	5	6.67
III	17	22.67
IV[a]	53	70.67
Metastatic lymph nodes (N:71)		
0–3	39	54.93
≥4	32	45.07
Radical operation (N:62)		
No	25	40.32
Yes	37	59.68
Primary tumor, sample type (N:75)		
Biopsy	6	8.00
Surgical specimen	69	92.00
Primary tumor, anatomical site (N:75)		
Left colon	60	80.00
Right colon [b]	15	20.00
Metastasis, sample type (N:75)		
Biopsy	18	24.00
Surgical specimen	57	76.00
Synchronous - metachronous metastases based on histology dates (N:75)		
Metachronous	42	56.00
Synchronous	33	44.00
Metastasectomy (based on histology reports[c] and clinical history, N:75)		
Yes	38	50.67
stage IV patients[c]	*18*	
nonstage IV patients	*20*	
No	37	49.33
Adjuvant treatment (N:19)		
Bevacizumab-containing	1	5.26
Chemotherapy only	18	94.74
1st line treatment (N:70)		
Bevacizumab-containing	43	61.43
Chemotherapy only	16	22.86
anti-EGFR containing	11	15.71

[a] For 20 of these patients, the available metastatic tissue was obtained at later time points.
[b] All these patients were stage IV.
[c] Synchronous metastasectomy in 5, relapse metastasectomy in 13 patients.

diagnosis. These corresponded to relapsed disease and were grouped together with the metastases obtained from non-stage IV patients for the purposes of this analysis. Thus, we examined 33 synchronous and 42 metachronous metastases, irrespectively of disease stage at diagnosis.

3.2. Histological and phenotypical characteristics

Typical examples of micronecrosis, tumor budding, and brisk TILs are shown in Fig. 2. High micronecrosis tended to coexist with high budding in primary tumors, although this association did not reach statistical significance. The number of tumor buds was weakly inversely correlated with TIL density in primary tumors (Spearman's rho = -0.2459; $P = 0.050$).

Primary and metastatic TILs were not associated with each other, either as continuous (Spearman's rho = 0.1298; $P = 0.2669$) or as categorical variables, nor within the subgroups of synchronous or metachronous metastases. Apart from micronecrotic areas in the primary tumor that were positively associated with higher positive nodal stage, no other histological variable was associated with the examined clinicopathologic parameters in the entire cohort.

The significant association between micronecrosis in primary/metastatic sites (Table 2) in fact applied to metachronous but was absent in synchronous metastases. Further statistical trends concerned more micronecrotic areas in metachronous metastases from patients of younger age, and more micronecrotic areas in synchronous metastases from patients with tumors in the right colon.

Finally, among the 58 tumors that were informative for MMR status with IHC (47 left and 11 right colon), there was only one MMR-deficient tumor (no expression of MSH6, MLH1, and PMS2 in both primary and metastasis). The patient, a 48year-old woman, presented with metastatic disease in the liver.

3.3. Genotypes

Missense variants classified as mutations were identified in 5 of 49 patients with informative germline DNA (for detailed description see DATA MANUSCRIPT). One of these germline variants was likely pathogenic based on ClinVar (*MSH6* p.Arg1076Cys) and was present in the matched primary tumor with preserved heterozygosity (52% VAF). Consistent with this finding, the respective tumor was MMR-deficient with IHC, as aforementioned. The genotype of the matched metastatic sample was noninformative.

In addition to the aforementioned, 433 tumor tissue mutations (381 unique variants across cases) were identified in 45 coding genes and were distributed in primary and/or metastatic samples from 64 of 75 patients (85.3%) (Fig. 3A). As anticipated [4], top mutated genes were *TP53* (60.0% of all cases and 70.3% of cases with mutations), *APC* (40.0% and 46.9%, respectively), and RAS genes, including *KRAS*, *NRAS,* and *HRAS* (40.0% and 46.9%, respectively). There were 9 cases (12.0% of all cases) with *PIK3CA* mutations in exon 9 and 20 hotspots; there were 14 cases (18.7%) with mutations in *EGF*, *EGFR*, *ERBB2*, *ERBB3,* or *ERBB4* (EGF/EGFR genes) and 11 cases (14.7%) with mutations in *MSH6* or *MSH3* (MMR genes).

Sixty-one (85.9%) primary tumors and 57 (81.4%) metastases carried 213 and 306 mutations in 37 and 42 genes, respectively. Mutations were identified in 56 of 66 (84.8%) cases eligible for genotype comparisons in matched primary/metastatic sites (Fig. 3B). The no-mutation status in primary tumors was preserved in all matched metastases (Fisher's $P < 0.0001$). The number of mutated genes was also significantly consistent in matched pairs (chi-square $P < 0.0001$); the overall Kappa coefficient was 0.60 (95% Confidence Interval (CI): 0.44−0.72; asymptotic Z-value <0.0001) and mostly concerned tumors without or with 1−2 mutated genes at both sites. By contrast, tumors with >10 mutated genes (4 primary, 6 metastatic) exhibited different alteration profiles at each site. Shared genomic alterations were found in 51 of 56 matched pairs with mutations (91.1%), more frequently in *TP53* (30 cases, 53.6%), RAS genes (22, 39.3%), and *APC* (17, 30.4%). Particularly *KRAS* mutations were not privately observed in primary tumors.

The mean/median VAFs in primary (26%/21%) and metastatic (23%/19%) sites did not differ, whereas there was a strong correlation between these values (Spearman's rho = 0.5665; $P < 0.0001$). Clonal mutations that are usually approached as tumor drivers were classified in 80.0% of all cases (73.2% of primary tumors and 67.1% of metastases); these were shared in 57.1% of comparable

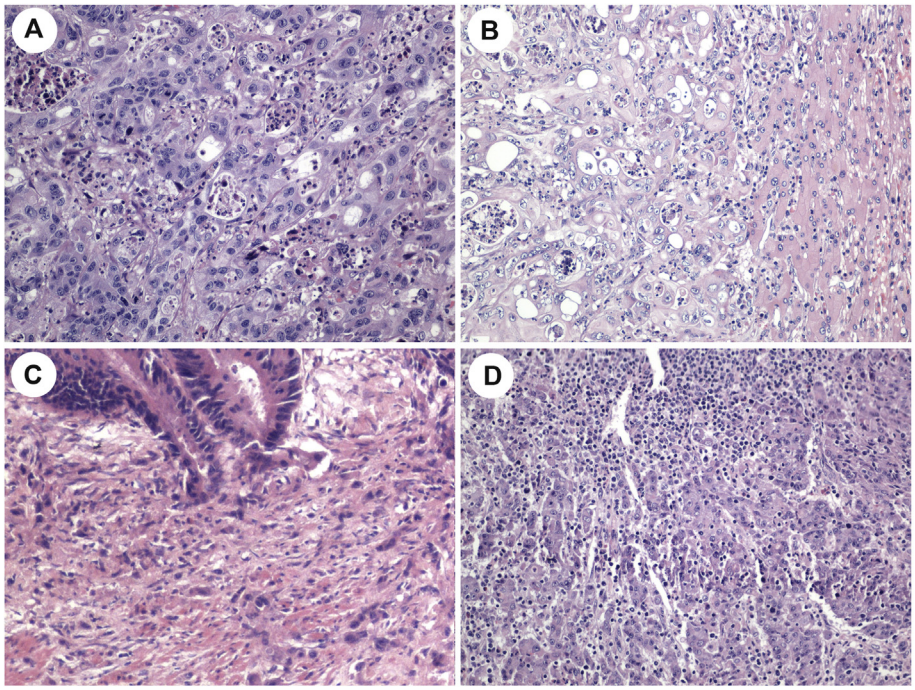

Fig. 2 Examples of the examined morphologic features. Hematoxylin and eosin (H&E) ×200 depicting increased number of micronecrosis areas in a primary tumor **(A)** and its paired metastasis **(B)**; increased tumor budding in the infiltrative front of a primary lesion **(C)**; brisk infiltrating lymphocytic reaction in a metastatic lesion **(D)**.

primary/metastatic pairs with mutations (Fig. 3A). Apart from *TP53*, *KRAS,* and *APC*, shared mutations in less frequently altered genes, e.g., *FBXW7*, *CDH1*, *AMER1*, *SOX9,* and in the EGF/EGFR genes, were predominantly clonal in either or both sites (Fig. 3C).

3.4. Genotype-phenotype associations

Associations of clinical and histological parameters with genomic alterations obtained with the Wilcoxon rank-sum test are presented in Fig. 4, those with chi-square in Table 3. High metastatic TILs were positively associated with the number of mutations and mutated genes in metastases (Fig. 4A), which was particularly in effect when 3 or more genes were mutated. In addition, high metastatic TILs significantly coincided with mutations in *KRAS* and all RAS genes, MMR genes, and *EGF* (Table 3). Interestingly, cases with *EGF* mutations had a significantly (Mann-Whitney $P < 0.001$) higher number of private mutations in metastases (median = 15) than *EGF* wild-type cases (median = 0). High-level micronecrosis in metastases was positively associated with *MSH6* and *APC* mutations (Table 3).

Compared with synchronous metastases, metachronous metastases exhibited higher numbers of private mutations (Fig. 4B); in addition, metachronous metastases less frequently shared clonal mutations with the primary tumor (Table 3). In the same line, more private mutations were detected in metastases from nonstage IV compared with those from stage IV patients (Fig. 4C).

Among metachronous metastases, those with high levels of TILs and micronecrosis had higher numbers of

Table 2 Histological parameters in primary and metastatic sites: significant associations in the entire cohort and within synchronous and metachronous metastatic subgroups.

Variable 1		Variable 2				Likelihood ratio *P*-value	Pearson's chi-square *P*-value	Fisher's exact test *P*-value
		N	%	N	%			
Micronecrosis primary	**Nodal status** Total compared: 68					0.0009[a]	0.0012[a]	0.0021[a]
		0-3 positive		≥4 positive				
	Low (0–9%)	20	54.05	5	16.13			
	High (≥10%)	17	45.95	26	83.87			
Micronecrosis primary	**Micronecrosis metastatic** Total compared: 66					0.018[a]	0.0178[a]	0.0216[a]
		Low (0–9%)		High (≥10%)				
	Low (0–9%)	14	56.0	11	26.8			
	High (≥10%)	11	44.0	30	73.2			
Micronecrosis metastatic, synchronous metastases	**Micronecrosis primary** Total compared: 25					0.8213	0.8213	>0.999
		Low (0–9%)		High (≥10%)				
	Low (0–9%)	5	41.7	6	46.2			
	High (≥10%)	7	58.3	7	53.8			
Micronecrosis metastatic, metachronous metastases	**Micronecrosis primary** Total compared: 41					0.0013[a]	0.0012[a]	0.0033[a]
		Low (0–9%)		High (≥10%)				
	Low (0–9%)	9	69.2	5	17.9			
	High (≥10%)	4	30.8	23	82.1			

TILs = tumor-infiltrating lymphocytes.
[a] Statistically significant associations.

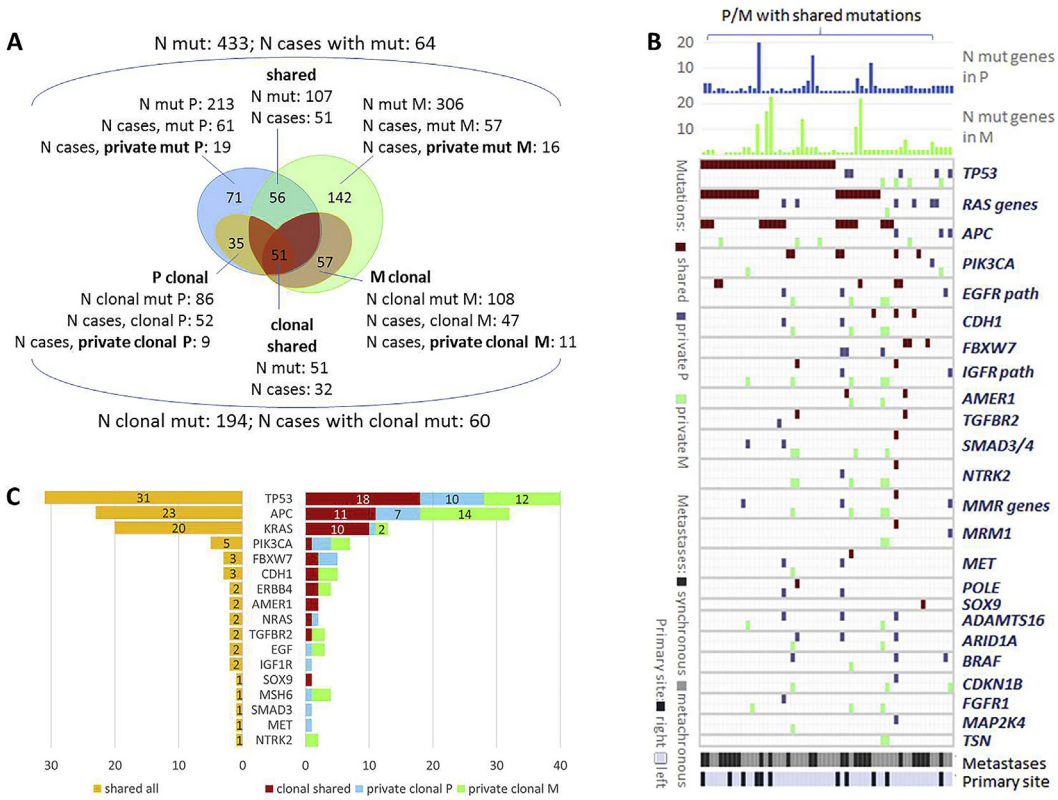

Fig. 3 Genotype characteristics of primary and matched metastatic tumors. (A) Venn diagram depicting the distribution (primary, metastatic) and type (shared, private, clonal, clonal shared, clonal private) of mutations; **(B)** Genotype comparison between primary and metastatic tumors. Shared and private primary or metastatic mutations in synchronous or metachronous metastases according to primary tumor location are presented. **(C)** Distribution of shared, clonal shared, and clonal private mutations in primary and metastatic lesions. Mut, mutation; P, primary; M, metastatic.

clonal mutations (Fig. 4D and E). Among synchronous metastases, those with high budding in the primary tumor did not exhibit private mutations (Fig. 4F).

3.5. Genotype and phenotype effects on patient outcome

The clinical end point in this study was obligatory OS. The examined cohort was small with respect to the number of examined patients and heterogeneous with respect to main parameters affecting colorectal cancer patient outcome, e.g., metastasectomy [11]. Single or profiled mutated genes examined per case or in either primary or metastatic site did not yield results pertaining to patient outcome, and the same applied to budding and micronecrosis. High TIL density in metastases favorably affected patient OS (Fig. 4G). Particularly patients with shared clonal mutations in primary/metastasis and with high metastatic TILs had the most favorable, whereas those with low metastatic TILs had the worst OS (Supplementary Fig. S1). TILs in the primary tumor were not associated with patient OS.

4. Discussion

4.1. Classic oncogenic driver mutations are frequently identified in primary and metastatic CRCs

Our study included informative genotype and phenotype data from matched primary and metastatic colorectal tumors. Genotyping showed the presence of mutations in classic oncogenic drivers such as *TP53*, *APC*, RAS genes, *PIK3CA,* and EGF/EGFR genes, which have been well studied in colorectal carcinogenesis [4]. In addition, we were able to identify interesting genotype-phenotype associations particularly regarding TILs and micronecrosis in metastatic tumors, which were insightful regarding tumor clonal evolution in metachronous metastases.

4.2. TILs in metastases are associated with specific genotype characteristics and are predictive of favorable OS

We showed that increasing TIL densities in metastases were associated with higher numbers of mutations and

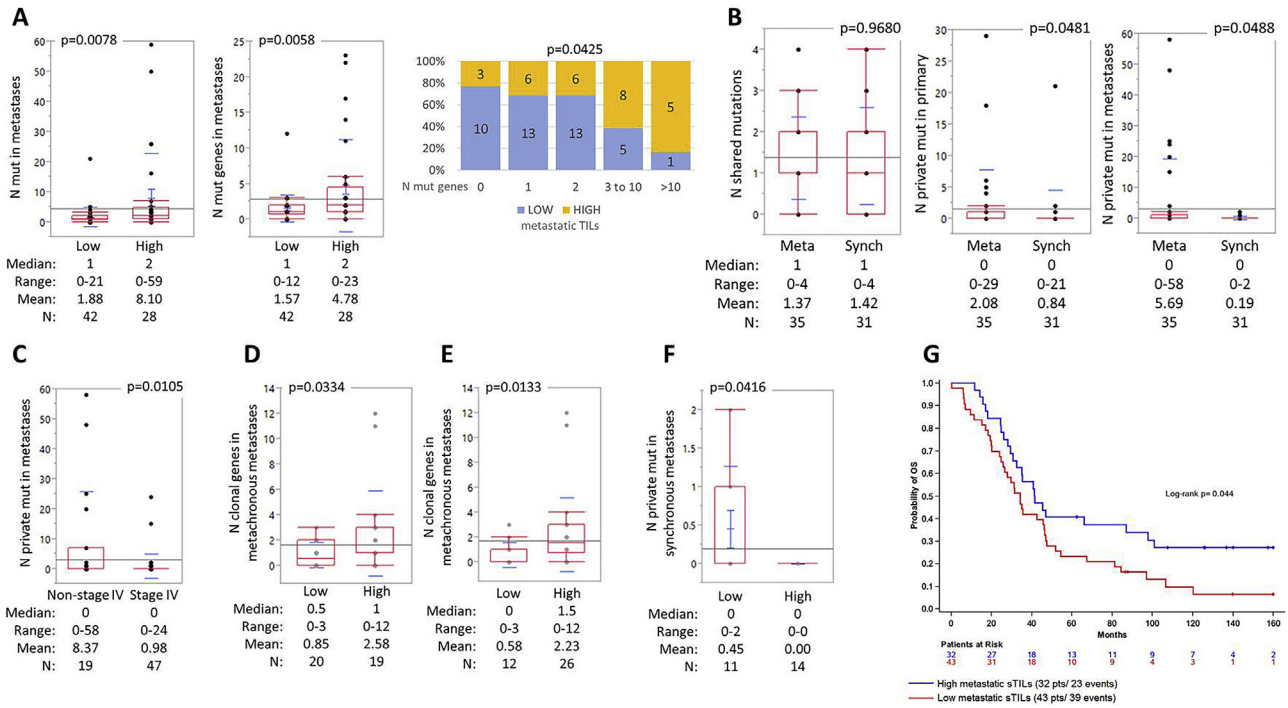

Fig. 4 Associations of phenotype with genotype characteristics and with patient outcome. **(A − F)** phenotype-genotype comparisons. Wilcoxon rank-sum test results are illustrated in box-plots; chi-square test (Pearson) in the bar chart in A. X-axes of box-plots in **A**, metastatic TIL density; in **B**, state of metastasis (synchronous or metachronous); in **C**, disease stage; in **D**, TILs in metachronous metastases; in **E**, level of micronecrosis in metachronous metastases; in **F**, budding in synchronous metastases. **G:** Kaplan-Meier curves showing favorable overall survival in patients with high TILs in the metastatic lesion. Mut, mutations; Meta, metachronous; Synch, synchronous; OS, overall survival; TILs, tumor-infiltrating lymphocytes.

mutated genes, prominently of the MMR and RAS families and *EGF*. TILs are considered to reflect a robust antitumor immune response [6] propagated and sustained by tumor neoantigens interacting with immune cells through major histocompatibility class I (MHC I) molecules [12]. This explains why brisk TIL responses are seen in MMR-deficient tumors, which accumulate an unusually high mutational burden resulting in increased neoantigen expression [13]. Further, in CRCs a subset of *KRAS* mutations can lead to production of neoepitopes recognized by CD4+ and CD8+ T-cells, as highlighted by Tran et al. [14] who described the immunogenic properties of $KRAS^{G12D}$ mutation in gastrointestinal cancers. This example and the present findings illustrate the close interaction between genotype and tumor immune response.

We highlighted that high TIL densities in metastatic tumors are associated with better OS. This effect was first reported by Okano et al. [15], in 2003, who concluded that high TILs in liver metastases from CRCs was an independent favorable prognosticator after metastasectomy. Similarly, Kwak et al. [16] used an immunoscore calculated from immunohistochemically assessed T cell subsets and tumor-infiltrating macrophages to show that the metastatic immunoscore was the only independent prognosticator, regardless of *KRAS* mutational status. Recently, Fuchs et al. [7] showed that morphologically assessed TILs are independent prognosticators of survival in colorectal cancer regardless of disease stage, MMR expression status, and *BRAF* mutational status.

TILs are also known to inversely associate with tumor budding mostly in right-sided MMR-deficient tumors that usually exhibit brisk TILs and low budding [13,17]. We were not able to demonstrate such an effect in our cohort that included only one tumor with documented MMR deficiency. On the other hand, we observed high levels of tumor budding in primary tumors lacking private mutations and exhibiting only shared ones with their synchronous metastases. This finding is in keeping with the aggressive biologic properties of tumors demonstrating high budding [17] and also with the described lack of barriers to the invasive properties of primary tumor clones in colorectal tumor growth [18]. In their review, Schumacher and Schreiber [19] discuss the origin of neoantigens deriving more often from private mutations and not from clonal − oncogenic ones. It is not surprising, therefore, that we identified higher frequencies of private mutations in metachronous metastases with higher TIL densities. In addition, because in our cohort *EGF*-

Table 3 Significant associations between histological parameters and genomic alterations.

Variable 1		Variable 2				Likelihood ratio	Pearson's chi-square (*P*-value)	Fisher's exact test (*P*-value)
		N	%	N	%			
Metastatic TILs	**RAS genes** Total compared: 75					0.0030*	0.0031*	0.0043*
		Nonmut		Mut				
	Low (0–19%)	32	71.1	11	36.7			
	High (≥20%)	13	28.9	19	63.3			
Metastatic TILs	***KRAS*** Total compared: 75					0.0172*	0.0172*	0.0244*
		Nonmut		Mut				
	Low (0–19%)	34	66.7	9	37.5			
	High (≥20%)	17	33.3	15	62.5			
Metastatic TILs	**MMR genes** Total compared: 75					0.0039*	0.0045*	0.0069*
		Nonmut		Mut				
	Low (0–19%)	41	64.1	2	18.2			
	High (≥20%)	23	35.9	9	81.8			
Metastatic TILs	***EGF*** Total compared: 75					0.0221*	0.0232*	0.0325*
		Nonmut		Mut				
	Low (0–19%)	41	62.1	2	22.2			
	High (≥20%)	25	37.9	7	77.8			
Micronecrosis metastatic	***MSH6*** Total compared: 68					0.0071*	0.0280*	0.0385*
		Nonmut		Mut				
	Low (0–9%)	26	42.6	0	0.0			
	High (≥10%)	35	57.4	7	100.0			
Micronecrosis metastatic	***APC*** Total compared: 68					0.0002*	0.0003*	0.0004*
		Nonmut		Mut				
	Low (0–9%)	22	56.4	4	13.8			
	High (≥10%)	17	43.6	25	86.2			
Synchronous vs. metachronous metastases	**Clonal mutations** Total compared: 56[a]					0.0176*	0.0194*	0.0291*
		Shared		Private				
	Metachronous	14	43.8	18	75.0			
	Synchronous	18	56.2	6	25.0			

TILs = tumor-infiltrating lymphocytes; mut = mutant; * Statistically significant associations.
[a] Comparison among paired samples with mutations, N = 56.

mutant metastases had more private mutations than *EGF* wild-type, it is reasonable that we observed higher TIL densities in the *EGF*-mutant subset of lesions. Previous comparative studies have shown high concordance of mutational status between primary colorectal tumors and their matched metastases [20,21]. However, it seems that the small subset of private mutations seen either in primary or metastatic lesions is biologically important for eliciting and propagating the host antitumor immune response [19].

4.3. Associations of micronecrosis with tumor genotypic characteristics

The term *micronecrosis* has been mostly used to describe microscopic foci of necrosis in meningiomas in a

background of aneuploidy [22]; such foci are adverse prognosticators of recurrence, implicative of aggressive biologic behavior [23]. Aneuploidy has been also associated with necrosis in other tumor types, notably renal cell carcinomas [24]. In addition to aneuploidy, a hypoxic tumor environment is also contributory to the development of both micronecrosis [25] and massive coagulative necrosis [26]. CRCs commonly harbor CNAs, particularly at the initial stages of tumorigenesis [27]. Persisting tumor subclones, dominating later on during the course of the disease, frequently have fewer CNAs because they have obtained an optimal aneuploidy status from an evolutionary perspective [27]. Nevertheless, CNAs are frequently found during all stages of colorectal cancer development [27], which may be part of the reason why we observed consistent levels of micronecrosis in primary tumors and their metastases. *APC* mutations seem to propagate the induction of CNA in colorectal tumors [28], which may explain why micronecrosis levels were high in metastatic tumors with *APC* mutations. Similarly, metastatic tumors with mutations in *MSH6* showed higher levels of micronecrosis which is in keeping with the focal necrosis seen in MMR-deficient tumors, rather than the typical *dirty* necrosis of microsatellite stable tumors [5]. Finally, although we did not address the presence of aneuploidy in our cohort, we demonstrated that primary tumors with high-level micronecrosis were clinically more aggressive since they were associated with higher positive nodal stage.

4.4. Metachronous metastases show genotypic evidence of tumor clonal evolution

We observed that metachronous metastases had more private mutations, particularly clonal mutations, than synchronous metastatic lesions. These findings fit well within the current understanding of clonal evolution in CRCs. As published, colorectal tumors have accumulated sufficient genetic aberrations to be capable of metastasizing very early during the course of disease; these tumors show high frequencies of shared mutations between primary and metastatic sites [21]. Regarding the development of metachronous metastases, Sun et al. [29] discuss the *Big Bang* model of clonal evolution according to which malignant tumors have already developed sufficient genomic alterations allowing them to continuously expand. These include private subclonal mutations which are initially undetectable due to dilution, but become evident later on, when a specific subclone persists and dominates. Our genotype findings in metachronous lesions are fully compatible with this model. Moreover, morphologic features such as brisk TILs and high-level micronecrosis could also be reflective of the distinctive molecular contexture in metachronous metastases; these observations are of potential clinical use because TILs and micronecrosis can be readily assessed on routine H&Es.

4.5. Study limitations

Our study was limited by the number of available cases (N = 75) and their heterogeneous basic clinical characteristics, which may explain our inability to detect a prognostic role for TILs and tumor budding in primary tumors. In addition, the small number of uncensored events limits the potential for unbiased multivariable analysis [30]. Collecting tissues from matched primary and metastatic CRCs can be challenging and most published studies contain numbers comparable with ours or lower [21]. The concept of micronecrosis is poorly studied outside of meningiomas [22] and pancreatic tumors [25]and strict distinction from massive coagulative necrosis is sometimes subjective and problematic [25]. Moreover, because both massive and microscopic necrosis arise in a background of hypoxia [25], it is unclear if they represent the same phenomenon or if microscopic necrosis is likely the effect of underlying genomic changes, as discussed above. Further experimental investigation will be useful to provide a better understanding of the biologic basis of micronecrosis in colorectal tumors. Finally, the group of metachronous metastases (N = 42) was heterogeneous regarding pretreatment status, and the number of cases was too small to allow for further subgroup analysis based on treatment data. Adjuvant treatment can interfere both with genotypic and phenotypic condition, mandating validation of our findings and further exploration with treatment subgroup analysis in a larger cohort.

5. Conclusions

In this study, we validated that mutations in classic oncogenic drivers such as *TP53, KRAS,* and *APC* are frequently shared between primary CRCs and their paired metastases. However, synchronous and metachronous metastases differ genotypically because metachronous metastases have more private and nonshared clonal mutations than synchronous. These genotype characteristics can explain the increased TIL densities and micronecrosis levels that we observed in metachronous. We also validated the favorable prognostic role of TILs in metastatic lesions. Our study highlights the importance of assessing certain histopathologic parameters on H&E sections, which often represent the harmonized outcome of complex molecular interactions [31]. If reproduced in larger case series, the assessment of TILs and micronecrosis in metastatic colorectal adenocarcinomas could be standardized as a practically no-cost procedure of prognostic clinical utility.

Acknowledgements

The authors are indebted to patients and their families for their trust and participation in the present registry. The authors thank Dr. Benjamin Van Treeck for his edits and

expert opinion, Emily Daskalaki for excellent technical assistance, and Maria Moschoni for coordination of data management.

Kyriakos Chatzopoulos: Conceptualization, Data curation, Investigation, Methodology, Validation, Visualization, Writing - original draft, Writing - review & editing; Vassiliki Kotoula: Conceptualization, Data curation, Formal analysis, Investigation, Methodology, Resources, Supervision, Validation, Visualization, Writing - original draft, Writing - review & editing; Georgia-Angeliki Koliou: Data curation, Formal analysis, Validation, Visualization, Writing - review & editing; Eleni Giannoulatou: Investigation, Methodology, Writing - review & editing; Kyriaki Papadopoulou: Investigation, Writing - review & editing; Vasilios Karavasilis: Resources, Writing - review & editing; Elissavet Pazarli: Resources, Writing - review & editing; Stavroula Pervana: Resources, Writing - review & editing; Georgia Kafiri: Resources, Writing - review & editing; Georgios Tsoulfas: Resources, Writing - review & editing; Sofia Chrisafi: Project administration, Writing - review & editing; Helen Sgouramali: Investigation, Writing - review & editing; Pavlos Papakostas: Resources, Writing - review & editing; Dimitrios Pectasides: Resources, Writing - review & editing; Prodromos Hytiroglou: Funding acquisition, Supervision, Writing - review & editing; George Pentheroudakis: Investigation, Resources, Supervision, Writing - review & editing; George Fountzilas: Conceptualization, Funding acquisition, Project administration, Resources, Supervision, Writing - review & editing.

Appendix A. Supplementary data

Supplementary data to this article can be found online at https://doi.org/10.1016/j.humpath.2020.10.009.

References

[1] Wild C, Weiderpass E, Stewart B. World cancer report: cancer research for cancer prevention. Lyon: International Agency for Research on Cancer; 2020.
[2] Siegel RL, Miller KD, Jemal A. Cancer statistics, 2017vol. 67. CA: Cancer J Clin; 2017. p. 7−30.
[3] Elferink MA, de Jong KP, Klaase JM, Siemerink EJ, de Wilt JH. Metachronous metastases from colorectal cancer: a population-based study in North-East Netherlands. Int J Colorectal Dis 2015;30:205−12.
[4] Cancer Genome Atlas N. Comprehensive molecular characterization of human colon and rectal cancer. Nature 2012;487:330−7.
[5] Hemminger JA, Pearlman R, Haraldsdottir S, et al. Histology of colorectal adenocarcinoma with double somatic mismatch-repair mutations is indistinguishable from those caused by Lynch syndrome. Hum Pathol 2018;78:125−30.
[6] Hendry S, Salgado R, Gevaert T, et al. Assessing tumor-infiltrating lymphocytes in solid tumors: a practical review for pathologists and proposal for a standardized method from the international immunooncology biomarkers working group: Part 1: assessing the host immune response, TILs in invasive breast carcinoma and ductal carcinoma in situ, metastatic tumor deposits and areas for further research. Adv Anat Pathol 2017;24:235−51.
[7] Fuchs TL, Sioson L, Sheen A, et al. Assessment of tumor-infiltrating lymphocytes using international TILs working group (ITWG) system is a strong predictor of overall survival in colorectal carcinoma: a study of 1034 patients. Am J Surg Pathol 2020;44:536−44.
[8] Lugli A, Kirsch R, Ajioka Y, et al. Recommendations for reporting tumor budding in colorectal cancer based on the International Tumor Budding Consensus Conference (ITBCC) 2016. Mod Pathol 2017;30:1299−311.
[9] Pollheimer MJ, Kornprat P, Lindtner RA, et al. Tumor necrosis is a new promising prognostic factor in colorectal cancer. Hum Pathol 2010;41:1749−57.
[10] Fountzilas E, Kotoula V, Pentheroudakis G, et al. Prognostic implications of mismatch repair deficiency in patients with nonmetastatic colorectal and endometrial cancer. ESMO Open 2019;4:e000474.
[11] Väyrynen V, Wirta EV, Seppälä T, et al. Incidence and management of patients with colorectal cancer and synchronous and metachronous colorectal metastases: a population-based study. BJS Open 2020;4(4):685−92.
[12] Jiang T, Shi T, Zhang H, et al. Tumor neoantigens: from basic research to clinical applications. J Hematol Oncol 2019;12:93.
[13] Halvarsson B, Anderson H, Domanska K, Lindmark G, Nilbert M. Clinicopathologic factors identify sporadic mismatch repair-defective colon cancers. Am J Clin Pathol 2008;129:238−44.
[14] Tran E, Ahmadzadeh M, Lu YC, et al. Immunogenicity of somatic mutations in human gastrointestinal cancers. Science 2015;350:1387−90.
[15] Okano K, Maeba T, Moroguchi A, et al. Lymphocytic infiltration surrounding liver metastases from colorectal cancer. J Surg Oncol 2003;82:28−33.
[16] Kwak Y, Koh J, Kim DW, Kang SB, Kim WH, Lee HS. Immunoscore encompassing CD3+ and CD8+ T cell densities in distant metastasis is a robust prognostic marker for advanced colorectal cancer. Oncotarget 2016;7:81778−90.
[17] van Wyk HC, Roseweir A, Alexander P, et al. The relationship between tumor budding, tumor microenvironment, and survival in patients with primary operable colorectal cancer. Ann Surg Oncol 2019;26:4397−404.
[18] Ryser MD, Mallo D, Hall A, et al. Minimal barriers to invasion during human colorectal tumor growth. Nat Commun 2020;11:1280.
[19] Schumacher TN, Schreiber RD. Neoantigens in cancer immunotherapy. Science 2015;348:69−74.
[20] Vakiani E, Janakiraman M, Shen R, et al. Comparative genomic analysis of primary versus metastatic colorectal carcinomas. J Clin Oncol 2012;30:2956−62.
[21] Hühns M, Krohn S, Murua Escobar H, Prall F. Genomic heterogeneity in primary colorectal carcinomas and their metastases: born bad or brought up a villain? Hum Pathol 2018;74:54−63.
[22] Cerdá-Nicolás M, López-Ginés C, Pérez-Bacete M, Barcia-Salorio JL, Llombart-Bosch A. Histopathological and cytogenetic findings in benign, atypical and anaplastic human meningiomas: a study of 60 tumors. Clin Neuropathol 2000;19:259−67.
[23] Kamei Y, Watanabe M, Nakayama T, Kanamaru K, Waga S, Shiraishi T. Prognostic significance of p53 and p21WAF1/CIP1 immunoreactivity and tumor micronecrosis for recurrence of meningiomas. J Neuro Oncol 2000;46:205−13.
[24] Dagher J, Dugay F, Verhoest G, et al. Histologic prognostic factors associated with chromosomal imbalances in a contemporary series of 89 clear cell renal cell carcinomas. Hum Pathol 2013;44:2106−15.
[25] Hiraoka N, Ino Y, Sekine S, et al. Tumour necrosis is a postoperative prognostic marker for pancreatic cancer patients with a high interobserver reproducibility in histological evaluation. Br J Canc 2010;103:1057−65.
[26] Couvelard A, O'Toole D, Leek R, et al. Expression of hypoxia-inducible factors is correlated with the presence of a fibrotic focus

and angiogenesis in pancreatic ductal adenocarcinomas. Histopathology 2005;46:668–76.
[27] Cross W, Kovac M, Mustonen V, et al. The evolutionary landscape of colorectal tumorigenesis. Nat Ecol Evol 2018;2:1661–72.
[28] Testa U, Pelosi E, Castelli G. Colorectal cancer: genetic abnormalities, tumor progression, tumor heterogeneity, clonal evolution and tumor-initiating cells. Med Sci 2018;6:31.
[29] Sun R, Hu Z, Curtis C. Big Bang tumor growth and clonal evolution. Cold Spring Harb Perspect Med 2018;8.
[30] Bradburn MJ, Clark TG, Love SB, Altman DG. Survival analysis Part III: multivariate data analysis – choosing a model and assessing its adequacy and fit. Br J Canc 2003;89:605–11.
[31] Rosai J. Why microscopy will remain a cornerstone of surgical pathology. Lab Invest 2007;87:403–8.